

Comparison of Two Lidar Methods of Wind Measurement by Cloud Tracking

JASON A. SANDERS, THOMAS D. WILKERSON

Utah State University, 1695 North Research Park Way, Logan, Utah 84341

GEARY K. SCHWEMMER, DAVID O. MILLER

Laboratory for Atmospheres, NASA Goddard Space Flight Center, Greenbelt, Maryland 20771

DAVID GUERRA

St. Anselm College, Manchester, New Hampshire, 03102

STEPHEN E. MOODY

Orca Photonic Systems, Inc., Redmond, Washington, 98052

ABSTRACT

We measured the horizontal wind speed vector with two separate lidar cloud tracking techniques. Data were taken during two measurement campaigns: HOLO-1, at Utah State University (USU), Utah, and HOLO-2 at St. Anselm College, New Hampshire. Army Research Office Lidar (AROL-2), Holographic Airborne Rotating Lidar Instrument (HARLIE), and a wide-angle camera were used during HOLO-1. Prototype Holographic Atmospheric Scanner for Environmental Remote Sensing (PHASERS) also participated in HOLO-2. Two measurement methods are described, and selected results from the two HOLO campaigns are shown.

1. Introduction

Two lidar research campaigns were conducted in 1999 to evaluate three new lidar instruments. The goal of the measurements was to evaluate the instruments' performance, develop data reduction routines, and explore scanning lidar applications. This paper emphasizes the measurement of the wind speed vector from data collected. The two campaigns were dubbed HOLO-1 and HOLO-2. HOLO-1 was conducted March 7, 1999, through March 13, 1999, at Utah State University's Space Dynamics Lab (SDL), in Logan, Utah. Three instruments were involved: the Holographic Airborne Rotating Lidar Instrument (HARLIE), Army Research Lidar (AROL-2), and a wide-angle monochrome CCD camera (SKYCAM). HARLIE, AROL-2, and SKYCAM were operated almost continuously for the entire campaign. The two lidars and the camera were set up on the roof of SDL. HOLO-2 was conducted June 5, 1999, through June 12, 1999, at St. Anselm College, in Manchester, New Hampshire. A third lidar instrument also took part in this campaign: Prototype Holographic Atmospheric Scanner for Environmental Remote Sensing (PHASERS) described by Guerra (1998) and Guerra *et al.* (1999). AROL-2, HARLIE, PHASERS, and the SKYCAM were operated almost continuously. AROL-2, HARLIE, and the SKYCAM were situated at the college's observatory, about 1 mile from the main campus.

2. Background

a. Lidar wind velocity measurements

Lidar wind vector measurements are based on the laser backscatter from clouds and aerosols. Several methods to measure the wind vector this way have been devised. Eloranta *et al.* (1975) used an elevation-scanning lidar pointed upwind to capture the shape and motions of aerosols and clouds as they pass through the lidar. Sasano *et al.* (1982) developed a scanning lidar method that determines the horizontal wind vector by matching aerosol distribution patterns. Sroga and Eloranta (1980) tracked aerosol particle distributions by scanning a lidar between three closely spaced small elevation azimuth angles. Pal *et al.* (1994) measured the wind speed from displacements in cloud features obtained from time-lapse video and simultaneous lidar altitude measurements. This method is also used in the present work by combining SKYCAM and AROL-2 data.

b. Instruments

Our wind speed measurements were derived from data taken with the AROL-2, HARLIE, and SKYCAM instruments. Table 1 lists the main properties of the two lidar systems. Orca Photonic Systems, Inc. built AROL-2 for Utah State University under a two-phase grant from the US Army Research Office. HARLIE, a holographic scanning lidar, was built at NASA's Goddard Space Flight Center (Schwemmer 1998). HARLIE scans the sky at a cone angle of 45° from the zenith. PHASERS was the original holographic lidar (Guerra *et al.* 1999).

Table 1. HARLIE and AROL-2 lidar properties.

	AROL-2	HARLIE
Wavelength (nm)	532	1064
Energy/Pulse (mJ)	100	2
Pulse Rate (Hz)	20	5000
Telescope Diameter (cm)	20	40
Range Resolution (m)	15	30
Data Channels	4	1
FOV Direction	Vertical	45° elevation

3. Methods

a. SKYCAM /AROL-2 method

Two methods were used to calculate the wind speed from the data collected during the two campaigns. The SKYCAM and the AROL-2 lidar were used together to establish the absolute size, direction of motion, and velocity of clouds during daytime observations (Pal *et al.* 1994). FIG 1 is a representative gray-scale display of AROL-2 cloud backscatter intensity, with altitude plotted vertically and time plotted to the right, for a three and a half hour period during HOLO-2 on June 6, 1999. Such cloud altitude data were combined with overhead cloud video images from SKYCAM to produce wind speed vector measurements. Only daytime observations are feasible with this method because the SKYCAM is not sufficiently sensitive for nighttime cloud photography.

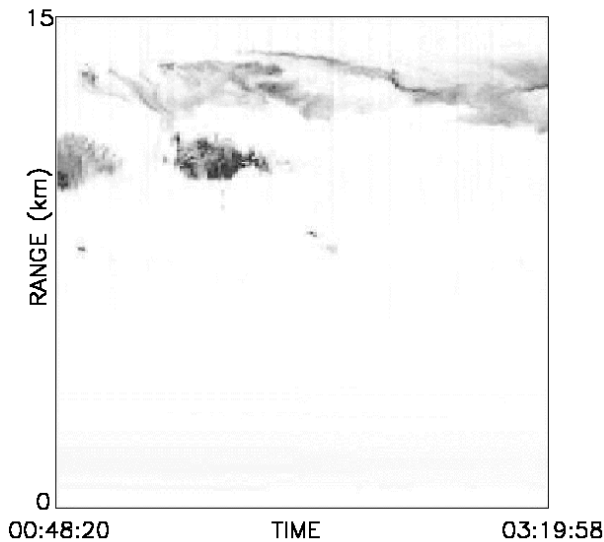


FIG. 1. AROL-2 data visualization plotting backscatter intensity as a function of range and time. Data taken from 12:48:20 A.M. to 3:19:58 A.M. on June 6, 1999, during the HOLO-2 campaign.

b. HARLIE method

The second method derives the wind speed vector from the HARLIE lidar data. FIG. 2 is a gray scale representation of the cloud backscatter data at an altitude of 2600 m collected by HARLIE during a 70-revolution scanning period lasting about 42 minutes on June 8, 1999, during HOLO-2. Time is in terms of the number of scan revolutions to the right, and the azimuthal angle (or scan angle) of observation is plotted vertically. In fact the full azimuthal extent is shown twice here for redundancy, so that the progress of cloud features across HARLIE's "cone of regard" can be visualized without having to match features occurring at 0° with those occurring at 360°.

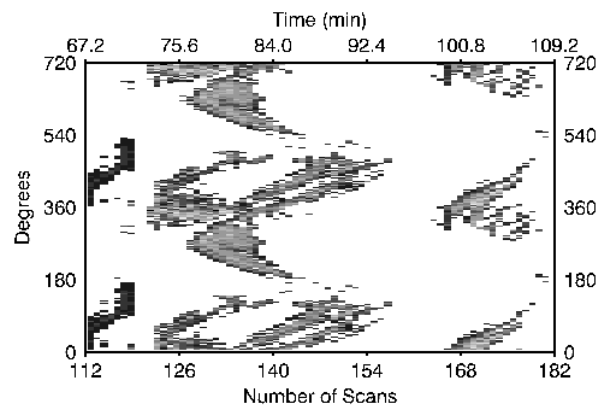


FIG. 2. HARLIE wave-image at 2600m taken during HOLO-2 on June 8, 1999, 10:40 P.M. to 11:22 P.M.

The use of such kinematic diagrams or "wave-images" facilitates the identification of the wind direction and the calculation of the wind speed. This calculation is aided by analyzing the simulated cloud field shown in FIG. 3, and its corresponding wave-image in FIG. 4.

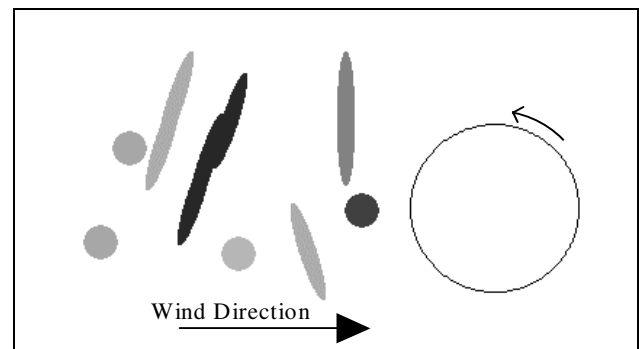


FIG. 3. A simulated cloud-field approaching a circle that represents the intersection of a HARLIE scan cone with the cloud altitude. The wind vector and scanner rotation direction are shown.

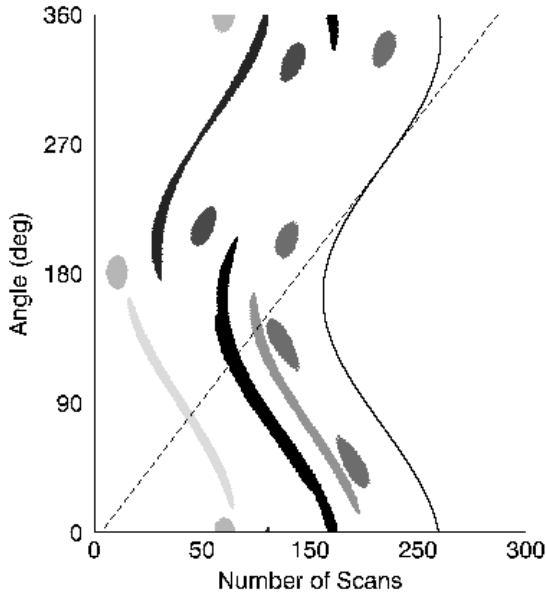


FIG. 4. The simulated wave-image corresponding to the cloud-field in FIG. 3. Note the wave-like behavior of the cloud features. A comparison arccosine function is plotted at the right. The dashed line, at the inflection point of the arccosine, provides the speed of the cloud features.

Clouds passing through the circle of a conical scanner with a speed v produce an arccosine curve in a wave image given by

$$\theta(n, v) = \arccos\left[\left(\frac{v \cdot n}{f \cdot R}\right) + \cos(\theta_i)\right], \quad (1)$$

where n is the number of revolutions, f is the frequency of revolution, R is the scanner radius, and θ_i is the initial scan angle. This function has been plotted alongside the simulated wave-image in FIG. 4.

The slope of (1) at the inflection point is

$$\frac{d\theta}{dn} = \frac{-v}{f \cdot R}, \quad (2)$$

from which one can find the wind speed of a cloud as it passes through the HARLIE scanning cone by evaluating the cloud's slope near the inflection point in a wave-image. The slope of the simulated wave-image is also plotted as a dashed line in FIG. 4.

FIG. 5. Shows a HARLIE wave-image with its slope line superimposed.

4. Results

Sample results of measuring the wind speed with both the SKYCAM /AROL-2 and the HARLIE-based methods are shown in Fig.6 and Fig.7 for data taken during HOLO-1 and HOLO-2, respectively. The two methods produce comparable results, with the statistical errors of the "wave image" method appearing to be significantly less than

those for the cloud imagery. A comprehensive summary of these comparisons is underway for the HOLO data and will be presented

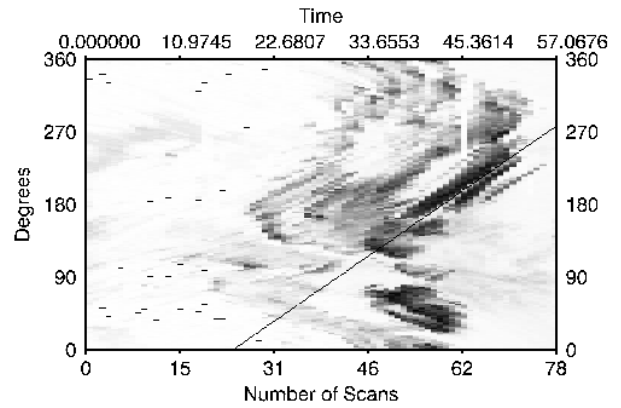


FIG. 5. A HARLIE wave-image with its corresponding slope-line superimposed. The wave image is of a cloud field at 2500m from 7:49 A.M. to 8:35 A.M. on March 10, 1999, during HOLO-1.

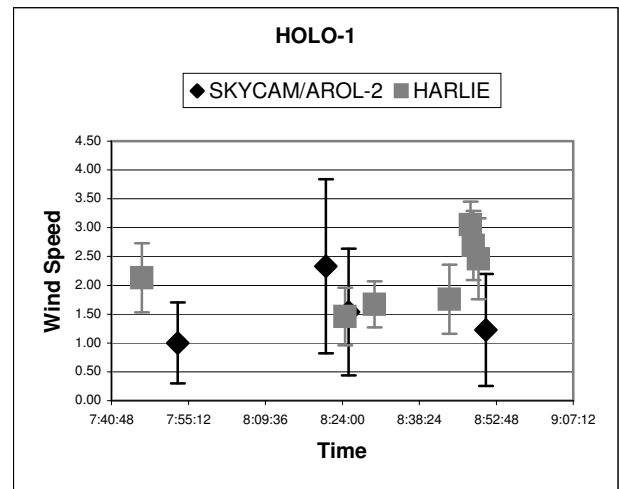


FIG. 6. Comparison chart of wind speeds, in meters per second, with the SKYCAM/AROL-2 and the HARLIE lidar systems. The data are taken from a one and a half hour period, on March 10, 1999, during the HOLO-1 measurement campaign.

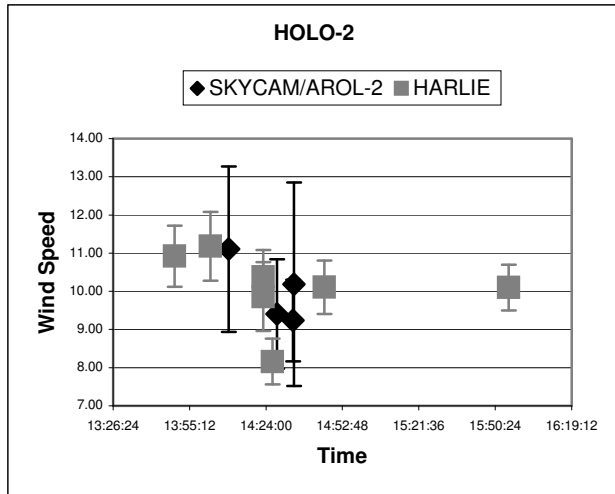


FIG. 7. Comparison chart of wind speeds, in meters per second, measured with the SKYCAM/AROL-2 and the HARLIE lidar systems. The data are taken during a three-hour period on June 8, 1999, from the HOLO-2 measurement campaign.

4. Acknowledgements

The Authors wish to acknowledge the National Aeronautics and Space Administration, Utah State University Space Dynamics Laboratory, US Army Research Office, and St. Anselm College for their support of this work.

REFERENCES

- Eloranta, E. W., J. M. King, and J. A. Weinmann, 1975: The Determination of Wind Speed in the Boundary Layer by Monostatic Lidar. *J. Appl. Meteor.*, **14**, 1485-1489.
- Guerra, D., 1998: Operation of the Prototype Holographic Atmospheric Scanner for Environmental Remote Sensing (PHASERS). *Proc. of the 19th International Laser Radar Conf.*, **2**, 879-882.
- Guerra, D. V., A. D. Wooten, S. S. Chaudhuri, G. K. Schwemmer, and T. D. Wilkerson, 1999. Prototype Atmospheric Scanner for Environmental Remote Sensing. *J. Geophys. Research*, **104**, 22,287-22,292.
- Pal, S. R., Pribluda, I. and Carswell, A. I., 1994: Lidar Measurements of Cloud-Tracked Winds. *J. Appl. Meteor.*, **35**, 35-44.
- Sasano, Y., Hirohara, H., Yamasaki, T., Shimizu, H., Takeuchi N. and Kawamura, T., 1982: Horizontal Wind Vector Determination from the Displacement of Aerosol Distribution Patterns Observed by a Scanning Lidar. *J. Appl. Meteor.*, **21**, 1516-1523.
- Schwemmer, Geary K., 1998: Holographic Airborne Rotating Lidar Instrument Experiment (HARLIE). *Proc. of the 19th International Laser Radar Conf.*, Annapolis, MD; NASA/CP-1998-207671/PT2, **2**, 623-626.
- Sroga, J. T. and Eloranta, E. W., 1980: Lidar Measurements of Wind Velocity Profiles in the Boundary Layer. *J. Appl. Meteor.*, **19**, 598-605.